Structural, Chemical, and Theoretical Evidence for the Electrophilicity of the $[C_6F_5Xe]^+$ Cation in $[C_6F_5Xe][AsF_6]$†

Hermann-J. Frohn,*,‡ Angela Klose,‡ Thorsten Schroer,‡ Gerald Henkel,§ Volker Buss,|| Daniel Opitz,|| and Rainer Vahrenhorst||

Gerhard-Mercator-Universität Duisburg, Lotharstrasse 1, D-47048 Duisburg, Germany

Received February 19, 1998

$[C_6F_5Xe][AsF_6]$ was prepared by metathesis from $[C_6F_5Xe][(C_6F_5)_2BF_2]$. The thermal stability of the melt (≤125 °C) is surprisingly high. The decomposition products reveal the ability of the cation to effect electrophilic pentafluorophenylation. $[C_6F_5Xe][AsF_6]$ crystallizes in the triclinic system, space group $P\bar{1}$, with four molecules in the unit cell. Of these, two are symmetry independent with Xe−C distances of 2.079(6) and 2.082(5) Å, Xe−F distances (cation−anion contacts) of 2.714(5) and 2.672(5) Å, and C−Xe−F angles of 170.5(3) and 174.2(3)°, respectively. The relation between cations and anions is best described as an asymmetric hypervalent (3c−4e) bond. Temperature dependent ^{19}F NMR measurements reveal the occurrence of separated ions in solution, with $[C_6F_5Xe]^+$ coordinated by a basic solvent molecule. Minimum energy geometries and charge distributions were calculated for $[C_6F_5Xe]^+$, $[C_6H_5Xe]^+$, $[C_6F_5]^+$, $[C_6H_5]^+$, $[CF_3Xe]^+$, $[CH_3Xe]^+$, $[C_6F_5Ng]^+$ (Ng = Kr, Ar, Ne, He), and $[C_6F_5Xe][AsF_6]$ at the ab initio RHF/LANL2DZ level. According to these calculations, C−Ng cations with short C−Ng distances are stable when the natural charge of the noble gas carries the main part of the positive net-charge and the *ipso*-C atom is not positive. In $[C_6F_5Xe]^+$, for example, 89% of the positive charge is concentrated on Xe.

Introduction

In all compounds containing an undisputed carbon−xenon bond Xe is bonded to a C−C fragment which contains a double or triple bond.[1] Most information is available for arylxenonium compounds, where the aryl group contains electron-withdrawing substituents.[2] For the synthesis of arylxenonium compounds two principle procedures are known. The introduction of aryl groups into XeF_2 by Lewis-acidic arylboranes (reaction 1) is a more common process than the electrophilic xenonylation of substituted benzenes (reaction 2).[3]

$$\underset{\mathbf{1}}{XeF_2} + \underset{\mathbf{2}}{(C_6F_5)_3B} \rightarrow \underset{\mathbf{3}}{[C_6F_5Xe][(C_6F_5)_2BF_2]} \quad (1)$$

$$XeF_2 \xrightarrow[\substack{1.\ 2(CF_3CO)_2O \\ 2.\ CF_3SO_3H}]{CCl_3F/-40\ ^\circ C} \xrightarrow{+1,3,5\text{-}C_6H_3F_3} [2,4,6\text{-}C_6H_2F_3Xe][CF_3SO_3] \quad (2)$$

According to eq 1 one aryl group of the borane **2** is transferred to Xe. The diaryldifluoroborate salt **3** is only stable at low temperature. The diaryldifluoroborate anion has two nucleophilic sites: the *ipso*-C of the aryl groups and the boron-bonded fluorine atoms. To stabilize the electrophilic arylxenonium cation at room temperature and higher temperatures, anions of weaker nucleophilicity than $[R_2BF_2]^-$ are necessary. Arylxenonium cations are weaker electrophiles than the fluoroxenonium cation $[FXe]^+$, **4**. In all compounds containing **4**, the cation is not isolated, but has close contact with the anion, and Xe is always linearly coordinated by fluorine and the nucleophilic site of the anion in an asymmetric hypervalent (3c−4e) arrangement.[4] Due to the reduced electrophilicity of $[C_6F_5Xe]^+$ relative to $[FXe]^+$ the interaction of arylxenonium cations with solvent molecules including organic solvents can be investigated more extensively than those of **4**.

First theoretical calculations on $[C_6H_5Ng]^+$ have been performed by Glaser[5] in order to compare $[C_6H_5N_2]^+$ with phenyl−

† This paper is dedicated to Prof. Bernt Krebs on occasion of his 60th birthday.

* Corresponding author.

‡ Fachgebiet Anorganische Chemie.

§ Fachgebiet Festkörperchemie.

|| Fachgebiet Theoretische Chemie.

(1) (a) Naumann, D.; Tyrra, W. *J. Chem. Soc., Chem. Commun.* **1989**, 47. (b) Frohn, H. J.; Jakobs, S. *J. Chem. Soc., Chem. Commun.* **1989**, 625. (c) Frohn, H. J.; Bardin, V. V. *J. Chem. Soc., Chem. Commun.* **1993**, 1072. (d) Zhdankin, V. V.; Stang, P. J.; Zefirov, N. S. *J. Chem. Soc., Chem. Commun.* **1992**, 578. (e) Frohn, H. J. *Nachr. Chem. Technol. Lab.* **1993**, *41*, 956.

(2) (a) Frohn, H. J.; Jakobs, S.; Henkel, G. *Angew. Chem.* **1989**, *101*, 1534. (b) Frohn, H. J.; Jakobs, S.; Rossbach, C. *Eur. J. Solid State Inorg. Chem.* **1992**, *29*, 729. (c) Butler, H.; Naumann, D.; Tyrra, W. *Eur. J. Solid State Inorg. Chem.* **1992**, *29*, 739. (d) Naumann, D.; Butler, H.; Gnann, R.; Tyrra, W. *Inorg. Chem.* **1993**, *32*, 861. (e) Frohn, H. J.; Rossbach, C. *Z. Anorg. Allg. Chem.* **1993**, *619*, 1672. (f) Gilles, T.; Gnann, R.; Naumann, D.; Tebbe, K.-F. *Acta Crystallogr.* **1994**, *C50*, 411. (g) Naumann, D.; Tyrra, W.; Pfolk, D. *Z. Anorg. Allg. Chem.* **1994**, *620*, 987. (h) Frohn, H. J.; Klose, A.; Henkel, G. *Angew. Chem.* **1993**, *105*, 114. (i) Naumann, D.; Gnann, R.; Padelidakis, V.; Tyrra, W. *J. Fluorine Chem.* **1995**, *72*, 79. (j) Frohn, H. J.; Klose, A.; Bardin, V. V. *J. Fluorine Chem.* **1993**, *64*, 201. (k) Frohn, H. J.; Schroer, T.; Henkel, G. *Z. Naturforsch.* **1995**, *50b*, 1799.

(3) (a) Naumann, D.; Tyrra, W.; Gnann, R.; Pfolk, D. *J. Chem. Soc., Chem. Commun.* **1994**, 2651. (b) Naumann, D.; Tyrra, W.; Gnann, R.; Pfolk, D.; Gilles, T.; Tebbe, K. F. *Z. Anorg. Allg. Chem.* **1996**, *623*, 1821.

(4) (a) Sladky, F. O.; Bulliner, P. A.; Bartlett, N. *J. Chem. Soc. A* **1969**, 2179. (b) Bartlett, N.; Gennis, M.; Gibler, D. D.; Morrell, B. K.; Zalkin, A. *Inorg. Chem.* **1973**, *12*, 1717.

S0020-1669(98)00190-6 CCC: $15.00
Published on Web 08/29/1998

noble gas cations. We have now studied the influence of fluorine substituents in the aryl group, the nucleophilicity of the counteranion and the nature of the noble gas on the stability of arylxenonium salts. In addition, the synthesis, the spectroscopic behavior and the crystal structure of $[C_6F_5Xe][AsF_6]$ are reported.

Experimental Section

Materials, Apparatus, and Methods. All reactions and NMR measurements were performed in FEP traps (3.5 or 8 mm i.d.) under a dry argon atmosphere unless mentioned otherwise. The thermal stability of **5** was investigated in a Netzsch M 404 DTA using stainless steel autoclaves for sample and reference. The melting point was measured in a sealed glass capillary with temperature correction. Reaction products and the ratios of the reaction products were determined by NMR spectroscopy. All solvents were dried using standard methods and were stored over molecular sieves (3 Å) prior to use. Literature methods were used for the syntheses of **3**,[2a] $(C_6F_5)_3B$,[6] AsF_5,[7] and $(C_6F_5)_2Cd$.[8]

Synthesis of $[C_6F_5Xe][AsF_6]$, 5. Method I. $(C_6F_5)_3B$ (4.0 g, 7.8 mmol) was dissolved in 150 mL of CH_2Cl_2 in a 250 mL flask. The solution was cooled to −50 °C, and XeF_2 (1.3 g, 7.8 mmol) was added to the vigorously stirred solution. After 3 h the formation of the colorless precipitate was finished. The suspension was cooled to −78 °C, the mother liquor was decanted, and the residue was suspended in 100 mL of CH_2Cl_2.

AsF_5 (0.57 mL condensed at −78 °C, 7.8 mmol) was vaporized and bubbled through the vigorously stirred suspension. After 10 min, the temperature was raised to room temperature (rt) and the reaction was continued for 30 min. After the slightly yellow precipitate had deposited, the CH_2Cl_2 solution of $(C_6F_5)_2BF$ was decanted and the residue was washed twice with 50 mL of CH_2Cl_2. The solid was dried in dynamic vacuum (0.1 hPa) for 8 h at rt resulting in 2.8 g (5.9 mmol) of pale yellow $[C_6F_5Xe][AsF_6]$.

Method II. **3** (789 mg, 1.16 mmol) was suspended in 50 mL of CH_2Cl_2 at −30 °C, and $AsF_5{\cdot}CH_3CN$ (244 mg, 1.16 mmol) was added to the stirred suspension. After 3 h, the CH_2Cl_2 solution of $(C_6F_5)_2BF{\cdot}MeCN$ was decanted and the residue was washed with 2 mL of CH_2Cl_2 at −30 °C twice and at rt eight times. The residue was dried in dynamic vacuum (0.1 h Pa) for 3 h, resulting in 457 mg (0.94 mmol) of pale yellow $[C_6F_5Xe][AsF_6]$.

Stability of $[C_6F_5Xe][AsF_6]$, 5, in the Solid State. Five samples of **5** (26−27 mg, 0.053−0.055 mmol) were filled in five autoclaves. The samples were heated (5 °C/min) to 125, 150, 167, 175, and 184 °C, respectively. The autoclaves were opened at −196 °C and 100 μL of CD_3CN was added. The autoclaves were closed and heated to rt. The CD_3CN solutions were investigated using ^{19}F NMR spectroscopy. The mixtures consisted of **5**, C_6F_6, and $AsF_5{\cdot}CD_3CN$. For the degree of decomposition at the different temperatures see Figure 1.

Stability of $[C_6F_5Xe][AsF_6]$, 5, in Solution. **5** was dissolved in MeCN, $MeNO_2$, H_2O, CF_3CH_2OH (TFE), SO_2, and anhydrous HF (aHF), respectively. In CD_3CN, **5** is stable for 12 h at rt. Total decomposition of **5** was observed after 35 days, resulting in C_6F_5D and $(C_6F_5)_2$ in the ratio of 6.7:1. At 80 °C the decomposition was complete after 4 h. The decomposition products consisted of C_6F_5H and $(C_6F_5)_2$ (12:1) in the case of CH_3CN and of C_6F_5D and $(C_6F_5)_2$ (6:1) in the case of CD_3CN, respectively. In H_2O, **5** decomposed completely after 72 h at rt and after 2 h at 80 °C. In aHF no decomposition of **5** could be observed at rt over months.

Reaction of $[C_6F_5Xe][AsF_6]$, 5, with $(C_6F_5)_2Cd$. **5** (46 mg 0.094 mmol) was suspended in a solution of 42 mg (0.094 mmol) of $Cd(C_6F_5)_2$ in 200 μL of CD_2Cl_2 at −40 °C. The suspension was stirred for 2 h at −40 and 0 °C and for 3 h at 40 °C. The mother liquor containing $(C_6F_5)_2$ (55 μmol), C_6F_5D (50 μmol), $(C_6F_5)_2AsF_3$ (38 μmol), $(C_6F_5)_3AsF_2$ (5 μmol), and $CDCl_2F$ (8 μmol) was decanted and the residue was dissolved in 200 μL CD_3CN. The residue consisted mainly of **5** and $Cd[AsF_6]_2$.

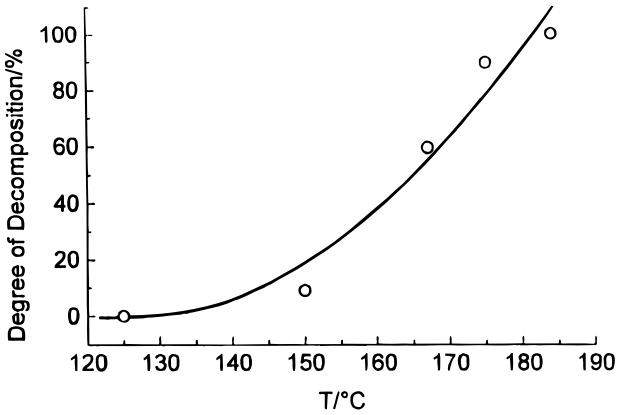

Figure 1. Course of thermal decomposition of $[C_6F_5Xe][AsF_6]$ in dynamic (5 °C/min) heating experiments.

Table 1. Crystallographic Data for $[C_6F_5Xe][AsF_6]$

chemical formula	$C_6F_{11}AsXe$
a [Å]	8.101(5)
b [Å]	8.241(5)
c [Å]	16.778(8)
α [deg]	94.07(3)
β [deg]	97.50(3)
γ [deg]	91.05(3)
V [Å^3]	1107.29
Z	4
fw [g mol^{-1}]	487.28
space group	$P\bar{1}$ (triclinic), No. 2
temperature [K]	150
λ (Mo K$_\alpha$) [Å]	0.710 73
ρ_{calcd} [g cm^{-3}]	2.923
μ(Mo Kα) [mm^{-1}]	6.21
transm range	0.981−0.377
$R = (\sum\|\|F_0\| - \|F_c\|\|)/\sum\|F_0\|$	0.0342
$R_w = [\sum w(\|F_0\| - \|F_c\|)^2/\sum wF_0^2]^{1/2}$	0.0420

Crystal Growth of $[C_6F_5Xe][AsF_6]$, 5. Single crystals of **5** were obtained by suspending **5** in CH_2Cl_2 at rt and adding CH_3CN until **5** dissolved completely. Slow vapor phase diffusion of CH_2Cl_2 led to the formation of single crystals of **5** over a period of 7 days.

Crystal Structure Determination of $[C_6F_5Xe][AsF_6]$, 5. The crystal was centered on a Siemens P4RA four-circle diffractometer equipped with a rotating anode tube and a graphite monochromator. Accurate cell dimensions were determined at 150 K from the setting angles of 18 centered reflections with $25 < 2\theta < 40°$. Integrated intensities were collected by the ω scan technique with scan rates varying from 6 to 30° and a scan range of ±0.5°. The data were collected within the range $4 < 2\theta < 54°$ (+h,±k,±l). During data collection the intensity of a standard reflection, monitored every 99 reflections, as well as all intensity profiles indicated stable measuring conditions. In total, 4840 reflections were collected of which 4336 were observed ($I > 2\sigma(I)$). An empirical absorption correction was applied, and corrections were made for Lorentz and polarization effects.

Solution and Refinement of the Structure. The structure was solved by direct methods (SHELXTL PLUS) in the triclinic space group $P\bar{1}$. The initial incomplete structural model was completed with difference Fourier techniques and refined (SHELXTL PLUS) taking into account anisotropic temperature factors for all atoms. The final refinement converged to $R = 0.0342$ and $R_w = 0.0420$. Crystallographic data for $[C_6F_5Xe][AsF_6]$ are given in Table 1.

NMR Spectroscopy. NMR spectra were recorded on a Bruker WP 80 SY pulse spectrometer equipped with an Aspect 2000 computer. For ^{19}F (75.39 MHz) a ∼90° pulse of 1.5 μs width was used. A total of 400 (800 for $Cs[AsF_6]$) transients was acquired in 32K memory using a spectral width setting of 10.2 kHz, an acquisition time of 1.6 s, a

(5) Glaser, R.; Horan, C. J. *J. Org. Chem.* **1995**, *60*, 7518.
(6) Pohlmann, J. L. W.; Brinckmann, F. E. *Z. Naturforsch.* **1965**, *20B*, 5.
(7) Ruff, O.; Menzel, W.; Plant, H. *Z. Anorg. Allg. Chem.* **1931**, *206*, 61.
(8) Schmeisser, M.; Weidenbruch, M. *Chem. Ber.* **1967**, *100*, 2306.

Table 2. ^{19}F NMR Data of $[C_6F_5Xe][AsF_6]$ and $[Cs][AsF_6]$ in CH_3CH_2CN/CD_3CN Solution at Different Temperatures (δ/ppm, J/Hz, $\Delta\nu_{1/2}$/Hz)

	$[C_6F_5Xe][AsF_6]$							$[Cs][AsF_6]$		
T/°C	δ F(2,6)	δ F(4)	δ F(3,5)	^3J(F−Xe)	δ $[AsF_6]^-$	^1J(F−As)	$\Delta\nu_{1/2}$	δ $[AsF_6]^-$	^1J(F−As)	$\Delta\nu_{1/2}$
32	−124.74	−141.40	−154.38	67.29	−64.63	933.2	66.5	−63.92	931.6	55.4
−1	−125.01	−141.54	−154.78	67.98	−64.69	930.2	86.5	−64.25	932.0	55.4
−20	−125.16	−141.61	−154.63	68.37	−64.66	930.4	98.1	−64.27	932.1	61.0
−40	−125.36	−141.70	−154.77	68.86	−64.67	932.2	126.4	−64.42	933.9	69.3
−60	−125.55	−141.79	−155.10	69.17	−64.67	924.6	176.3	−64.54	932.9	77.6
−80	−125.76	−141.87	−154.97	69.54	−64.57	904.3	402.5	−64.55	931.1	123.4

relaxation delay time of 2 s, and a resolution of 0.62 Hz/data point. The free induction decays were multiplied by a Gaussian function using a line broadening of 0.6 Hz. Shift values are referred to CCl_3F using C_6F_6 as internal standard or as primary reference in the appropriate solvent at the appropriate temperature with C_6F_6 ($\delta = -162.9$ ppm). For ^{129}Xe (22.22 MHz) a ~90° pulse of 3.0 μs width was used. A total of 600 transients was acquired in 16K memory using a spectral width setting of 20 kHz, an acquisition time of 0.4 s, a relaxation delay time of 1 s, and a resolution of 2.44 Hz/data point. The free induction decays were multiplied by a Gaussian function using a line broadening of 2.4 Hz. $XeOF_4$ (neat, 24 °C) was used as an external standard ($\delta = 0$ ppm) and XeF_2/MeCN/24 °C ($c \rightarrow 0$) as secondary reference: XeF_2 ($\delta = -1813.28$ ppm).

NMR Data of $[C_6F_5Xe][AsF_6]$, 5, in Different Solvents. For ^{19}F NMR spectroscopy approximately 30 mg (0.06 mmol) of **5** was dissolved in 200 μL of the appropriate solvent (see Table 5). For the ^{129}Xe NMR spectra 100 mg (0.21 mmol) of **5** was dissolved in 2 mL of CD_3CN and 2 mL of a saturated solution were used in the case of D_2O, respectively (see Table 5).

NMR Spectra of $[C_6F_5Xe][AsF_6]$, 5, in CH_3CH_2CN/CD_3CN (3:1) at Different Temperatures. A 30 mg (0.06 mmol) amount of **5** was dissolved in a mixture of 225 μL of CH_3CH_2CN and 75 μL of CD_3CN. ^{19}F NMR spectra were obtained at 32, −1, −20, −40, −60, and −80 °C. The same procedure was carried out with a saturated solution of $Cs[AsF_6]$ in this solvent mixture (see Table 2).

Computational. Standard Hartree−Fock ab initio molecular orbital calculations were performed with the GAUSSIAN 94 program package.[9] Optimized geometries were obtained at the RHF/LANL2DZ level except for He and its compounds where a 6-31G base was employed. Standard geometries were used as starting points for the structure optimization, which were performed without any symmetry restrictions. Atomic charges were calculated using both the Mulliken and the natural population analysis (NPA) as implemented in the NBO program.[10]

Results and Discussion

Synthesis and Properties of $[C_6F_5Xe][AsF_6]$. $[C_6F_5Xe][AsF_6]$, **5**, was obtained by the reaction of **3** with gaseous AsF_5 or solid $AsF_5 \cdot CH_3CN$ in CH_2Cl_2 suspension (eqs 3 and 4). These syntheses demonstrate a general procedure with arylxenonium fluoroborates as starting materials. In the anion of **3** the fragment $(C_6F_5)_2BF$ can be replaced by stronger Lewis acids such as AsF_5. $[C_6F_5Xe]^+$, $(C_6F_5)_2BF$, and AsF_5 are competing for the charged and hard base F^-. At the end of reaction 4 the noncharged and softer base MeCN is coordinated with the borane.

$$\underset{\mathbf{3}}{[C_6F_5Xe][(C_6F_5)_2BF_2]}\downarrow + AsF_{5(g)} \xrightarrow{CH_2Cl_2} \underset{\mathbf{5}}{[C_6F_5Xe][AsF_6]}\downarrow + (C_6F_5)_2BF \quad (3)$$

$$[C_6F_5Xe][(C_6F_5)_2BF_2]\downarrow + AsF_5 \cdot MeCN \xrightarrow{CH_2Cl_2} [C_6F_5Xe][AsF_6]\downarrow + (C_6F_5)_2BF \cdot MeCN \quad (4)$$

5 is a slightly yellow solid which can be stored for a prolonged period at room temperature under an inert atmosphere without decomposition. It melts at 102 °C forming a viscous liquid. Dynamic heating experiments (5 °C/min) show that the melt is thermally stable until 125 °C. Slow decomposition takes place between 125 and 180 °C (Figure 1) with electrophilic transfer of the C_6F_5 group to one fluoride ion of the fluoroelementate anion (eq 5).

$$[C_6F_5Xe][AsF_6] \xrightarrow{\Delta} C_6F_6 + AsF_5 + Xe^\circ \quad (5)$$

5 can be dissolved at ambient temperature in solvents such as MeCN, $MeNO_2$, H_2O, CF_3CH_2OH (TFE), SO_2, and anhydrous HF (aHF). The stabilities of these solutions differ markedly. In MeCN **5** shows no decomposition at rt over 12 h but is totally decomposed after 35 days. At 80 °C total decomposition takes place in 4 h. In H_2O **5** is less stable and total decomposition is observed at rt after 3 days and at 80 °C after 2 h.

The influence of the donor number DN, the acceptor number AN and the dielectric constant ϵ on the dissolution behavior of **5** and of the ionization potential IP on the stability of solutions of **5** can be elucidated by comparing MeCN (DN = 18.9,[11] AN = 14.1,[11] ϵ = 37.5,[12] IP = 12.2[13]) and Et_2O (DN = 19.2,[11] AN = 3.9,[11] ϵ = 4.3,[12] IP = 9.6[13]). Cation−anion separation and anion coordination are less favored in Et_2O. Below −40 °C **5** is practically insoluble in Et_2O, and above this temperature dissolution with spontaneous decomposition results in the formation of C_6F_5H. For the slow decomposition in MeCN at rt with formation of C_6F_5H and $C_6F_5-C_6F_5$ a significant isotopic effect is observed. The ratio in MeCN is 12:1 for C_6F_5H:$(C_6F_5)_2$, while in CD_3CN the ratio C_6F_5D:$(C_6F_5)_2$ is 6.7:1. For the reaction two alternatives can be envisaged both with species

(9) Frisch, M. J.; Trucks, G. W.; Schlegel, H. B.; Gill, P. M. W.; Johnson, B. G.; Robb, M. A.; Cheeseman, J. R.; Keith, T.; Petersson, G. A.; Montgomery, A.; Raghavachari, K.; Al-Laham, M. A.; Zakrzewski, V. G.; Ortiz, J. V.; Foresman, J. B.; Peng, C. Y.; Ayala, P. Y.; Chen, W.; Wong, M. W.; Andres, J. L.; Replogle, E. S.; Gomperts, R.; Martin, R. L.; Fox, D. J.; J. Binkley, S.; Defrees, D. J.; Baker, J.; Stewart, J. J. P.; Head-Gordon, M.; Gonzalez, C.; Pople, J. A. *GAUSSIAN 94.*, Revisions B.1 and B.3; Gaussian Inc.: Pittsburgh, PA, 1995.

(10) (a) NBO, Version 3.1; Glendening, E. D.; Reed, A. E.; Carpenter, J. E.; F. Weinhold. (b) Foster, J. P.; Weinhold, F. *J. Am. Chem. Soc.* **1980**, *102*, 7211. (c) Reed, A. E.; Weinstock, R. B.; Weinhold, F. *J. Chem. Phys.* **1985**, *83*, 735. (d) Reed, A. E.; Weinhold, F. *J. Chem. Phys.* **1985**, *83*, 1736.

(11) Griffiths, T. R.; Pugh, D. C. *Coord. Chem. Rev.* **1979**, *29*, 129.

(12) Watanabe, K.; Nakayama, T.; Mottl, J. *J. Quant. Spectrosc. Radiat. Transfer* **1962**, *2*, 369.

(13) Solouki, B.; Bock, H. *Chem. Ber.* **1975**, *108*, 897.

Table 3. Selected Distances and Angles of $[C_6F_5Xe][AsF_6]$

	distance/Å		bond angle/deg		interatomic distance/Å	
molecule 1	C(1)−Xe(1)	2.079(6)	C(1)−Xe(1)−F(1)	170.5(3)	F(13)−Xe(1)	3.129(5)
	Xe(1)−F(1)	2.714(5)	Xe(1)−F(1)−As(1)	126.4(3)	F(17)−Xe(1)	3.142(5)
	F(1)−As(1)	1.748(3)	C(2)−C(1)−C(6)	121.5(5)	F(2)−Xe(1)	3.347(5)
	F(4)−As(1)	1.707(3)				
	F−As(1)[a]	1.713(3)				
molecule 2	C(7)−Xe(2)	2.082(5)	C(7)−Xe(2)−F(7)	174.2(3)	F(18)−Xe(2)	3.120(5)
	Xe(2)−F(7)	2.672(5)	Xe(2)−F(7)−As(2)	128.7(3)	F(22)−Xe(2)	3.144(5)
	F(7)−As(2)	1.743(4)	C(8)−C(7)−C(12)	122.4(5)	F(8)−Xe(2)	3.423(5)
	F(10)−As(2)	1.700(4)				
	F−As(2)[a]	1.705(4)				

[a] Average length of the F_e−As distances.

with an asymmetric hypervalent C−Xe bond as intermediates (see reactions a and b).

a

$$[C_6F_5Xe{\cdot}NCMe]^+ \rightarrow C_6F_5^{\bullet} + {}^{\bullet}Xe{-}NCMe^+ \text{ or } C_6F_5Xe^{\bullet} + MeCN^{\bullet+}$$

b

$$[C_6F_5Xe{\cdot}NCMe]^+ + F^- \rightarrow C_6F_5{-}Xe{-}F \rightarrow C_6F_5^{\bullet} + {}^{\bullet}Xe{-}F$$

$$2C_6F_5^{\bullet} \rightarrow (C_6F_5)_2$$

$$C_6F_5Xe{\cdot}F{-}AsF_5 \xrightarrow[-\ AsF_5]{MeCN} C_6F_5{-}Xe{-}F \rightarrow C_6F_5^{\bullet} + {}^{\bullet}Xe{-}F$$

Alternative b, in which F^- comes from the solvolysis of $[AsF_6]^-$ and in which the leaving electrophile AsF_5 forms an adduct with the basic solvent, seems to be favored, because **5** reacts in MeCN after addition of CsF in a fast reaction and shows a similar isotopic effect and forms the same products as in the above decomposition.[14]

Molecular Structure. **5** crystallizes from a CH_2Cl_2−MeCN solution by CH_2Cl_2 diffusion at room temperature in the triclinic system (space group $P\bar{1}$) with four formula units per unit cell. The cell contains two crystallographically independent molecules (Figure 2, Table 3). In both molecules one fluorine atom of $[AsF_6]^-$ forms a bridge to the electrophilic Xe center. Consequently, Xe is involved in a near linear C−Xe−F_b asymmetric hypervalent bonding situation. There is a relation between the distance of bridging atom F_b of $[AsF_6]^-$ and Xe and the Xe−C distance: when the former gets shorter, the latter gets elongated (compare molecules 1 and 2). This effect is more pronounced in $C_6F_5XeO_2CC_6F_5$[2h] with the more nucleophilic anion. Thus, weak anionic nucleophiles behave similarly to the neutral nucleophiles in $[C_6F_5Xe{\cdot}NCMe]^+$ [2a] and $[C_6F_5Xe{\cdot}NC_5H_3F_2\text{-}2,6]^+$ [2k] (Table 4).

In addition to the asymmetric hypervalent bond in **5**, there are two types of Xe−F contacts shorter than the sum of van der Waals radii[15] (3.47 Å) in each molecule: one contact between an equatorial As-bonded F atom and Xe caused by the nonlinear Xe−F_b−As arrangement and two forced contacts of the F atoms in the ortho-positions of the C_6F_5 group. In both molecules of **5** the Xe−F_b distance is shorter than in $[2,6\text{-}C_6H_3F_2Xe][BF_4]$,[2f] despite the more nucleophilic $[BF_4]^-$ anion. The unexpectedly long Xe−F_b distance in $[2,6\text{-}C_6H_3F_2Xe][BF_4]$ is explained by our computational results below.

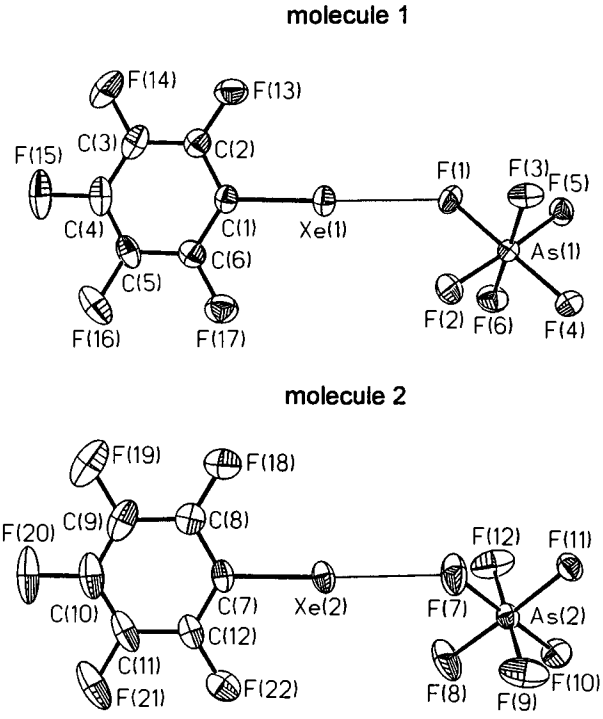

Figure 2. Molecular structure of $[C_6F_5Xe][AsF_6]$ with the characteristic linear coordination of Xe(II).

NMR Spectroscopy. To enlarge the temperature range below the melting point of MeCN a 1:3 mixture of MeCN and EtCN was used. With decreasing temperature the ^{19}F NMR chemical shift δ F(4) moves to lower frequencies and $^3J_{F,Xe}$ increases (see Figure 3), both in a linear manner. In addition, the line width of the $[AsF_6]^-$ resonance in **5** becomes larger by a factor of 3 compared to $Cs[AsF_6]$ at −80 °C.

From studies of the coordination of pyridines of different basicity to $[C_6F_5Xe]^+$, it is known that $^3J_{F,Xe}$ increases and δ F(4) shifts to lower frequency with stronger coordination.[2k] This information allows us to interpretate the temperature dependence of the observed NMR values. At lower temperature the anionic nucleophile $[AsF_6]^-$ tends to replace the neutral nucleophile MeCN in the coordination sphere of $[C_6F_5Xe]^+$.

$$[C_6F_5Xe{\cdot}NCMe]^+ + [AsF_6]^- \rightleftharpoons [C_6F_5Xe{\cdot}F_b{-}AsF_5] + MeCN \quad (6)$$

Coordination of the $[AsF_6]^-$ anion lowers the octahedral symmetry and causes broadening of the anion signal. We assume that in MeCN solution the coordination at the xenon center is comparable to the situation in the solid state,[2a,f,k] with asymmetric hypervalent coordination to the C−Xe fragment by the N or F base.

(14) Frohn, H. J.; Klose, A.; Bardin, V. V.; Kruppa, A. J.; Leshina, T. V. *J. Fluorine Chem.* **1995**, *70*, 147.
(15) Bondi, A. *J. Phys. Chem.* **1964**, *68*, 441.

Table 4. Structural Comparison of $C_6F_5Xe^+$ Compounds

compound	ref	distances/Å		angles/deg	
		C_i-Xe	$Xe-nu$	$C_i-Xe-nu$	$C-C_i-C$
$C_6F_5Xe\cdot F_b-AsF_5$ (1)[a]		2.079(6)	2.714(5)	170.5(3)	121.5(5)
$C_6F_5Xe\cdot F_b-AsF_5$ (2)[b]		2.082(5)	2.672(5)	174.2(3)	122.4(5)
$C_6F_5Xe\cdot OC(O)C_6F_5$[c]	2h	2.122(4)	2.367(3)	178.1(1)	119.2(3)
$[C_6F_5Xe\cdot NCMe]^+$	2a	2.092(8)	2.681(8)	174.5(3)	122.9(7)
$[C_6F_5Xe\cdot NC_5H_3F_2-2,6]^+$	2k	2.087(5)	2.694(5)	180.0(1)	121.9(5)

[a] ∠Xe−F_b−As: 126.4(3)°. [b] ∠Xe−F_b−As: 128.7°. [c] ∠Xe−O−C: 112.2(2)°.

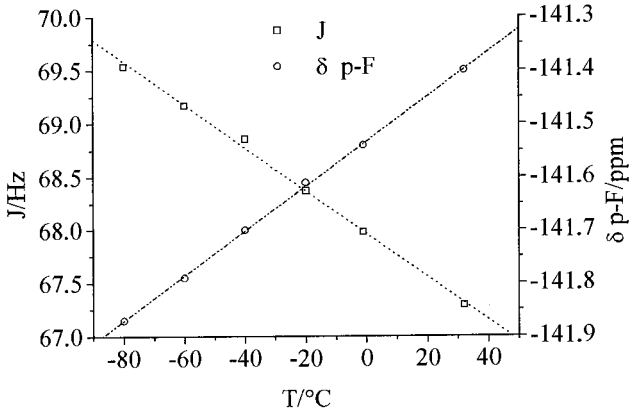

Linear Regression:

$J = A + B \cdot T$

$A = 67.96 \pm 0.025$ Hz

$B = -0.0203 \pm 0.00055$ Hz °C^{-1}

$r = -0.99851$

Linear Regression:

δ p-F $= A + B \cdot T$

$A = -141.533 \pm 0.0024$ ppm

$B = 0.00421 \pm 0.00005$ ppm °C^{-1}

$r = 0.99971$

Figure 3. Linear temperature dependence of the ^{19}F NMR shift value δ/ppm of the *p*-F atom and of $^3J_{F,Xe}$/Hz of $[C_6F_5Xe][AsF_6]$ dissolved in a 1:3 mixture of MeCN and EtCN.

The different possibilities of interaction of the electrophilic cation in solutions of **5** (cation−solvent vs cation−anion) and the intensity of interaction with different solvents can be monitored by heteronuclear NMR. We have found no solvent in which **5** is dissolved as molecule. The polarity of **5** with its strong interaction between the cationic and anionic part requires polar solvents. Experimentally it was found that only solvents with high DN or AN and additionally ϵ values larger than 15 dissolve **5**. Under these conditions cation−anion separation is mainly favored. Solvents of high nucleophilicity (MeCN, H_2O) coordinate to the cation of **5** and are responsible for the low-frequency shifts of F(4) and large $^3J_{F,Xe}$ coupling constants. In aHF (superacidic conditions) we have a weak coordination of the cation combined with the strong solvation of the anion. The cation exhibits the highest frequency for F(4) and the smallest $^3J_{F,Xe}$ value. SO_2 and TFE have borderline character (Table 5). A short and strong contact of the nucleophile causes a large $^3J_{F,Xe}$ coupling.[2h] The observed shift of F(4) can be explained by the different polarization ability of Xe(II) or rather Xe(II)-nucleophile on the C_6F_5 moiety. More detailed arguments concerning the electron density of the C_6F_5Xe fragment are discussed in the theoretical treatment.

Chemical Proof of the Cation−Anion Interaction in $[C_6F_5Xe][AsF_6]$, 5. We used the reactivity of the $[AsF_6]^-$ anion in the fluorine-aryl substitution reaction with $Cd(C_6F_5)_2$ as an indicator of the $[AsF_6]^-$ polarization by the cation in the case of **5**. The nonpolarized $[AsF_6]^-$ in $[NMe_4][AsF_6]$ does not react with $Cd(C_6F_5)_2$ in MeCN solution at rt despite the nucleophilic activation of the aryl group by the basic solvent. **5** reacts completely with $Cd(C_6F_5)_2$ in CD_2Cl_2 suspension up to 40 °C with formation of C_6F_5D, $(C_6F_5)_2$, $(C_6F_5)_2AsF_3$, $(C_6F_5)_3AsF_2$, and $CDCl_2F$. The different reactivity of $[AsF_6]^-$ in these cases can be explained by the cation−anion interaction in solid **5** mentioned before.

$$C_6F_5Xe\cdot F_b-AsF_5 + Cd(C_6F_5)_2 \xrightarrow{CD_2Cl_2} (C_6F_5)_2AsF_3 + CdF_2 + \langle C_6F_5XeF\rangle$$

$$\langle C_6F_5XeF\rangle \rightarrow C_6F_5^{\bullet} + FXe^{\bullet}$$

$$C_6F_5^{\bullet} \xrightarrow{CD_3CN} C_6F_5D + (C_6F_5)_2$$

Computational Results. To better understand the structural features and reactivity of **5**, we have carried out ab initio calculations (RHF level, LANL2DZ basis set, except for He and its compounds, where a 6-31G base was employed) on $[C_6F_5Xe][AsF_6]$ (**5**), $[C_6F_5Xe]^+$ (**6**), $[C_6F_5]^+$ (**7**), $[C_6H_5Xe]^+$ (**8**), $[C_6H_5]^+$ (**9**), $[2,6\text{-}C_6H_3F_2Xe]^+$ (**10**), $[CF_3Xe]^+$ (**11**), $[CH_3Xe]^+$ (**12**), and $[C_6F_5Ng]^+$ [Ng = Kr (**13a**), Ar (**13b**), Ne (**13c**), He (**13d**)]. Pertinent results are given in Tables 6 and 7.

Xe−C bond formation, as in **6**, can be described formally as recombination of the $[C_6F_5]^{\bullet}$ radical with the $Xe^{\bullet+}$ radical cation or alternatively as polarization of Xe° by $[C_6F_5]^+$. The latter appears to be more realistic since according to the population analysis (both Mulliken and NBO), the positive charge in **6** is centered on Xe. Obviously the C_6F_5 group is able to withstand the positively charged Xe atom. The σ backbone of the C_6F_5 group is electron-poor due to the five terminal F atoms. As a consequence, there is only a small positive σ charge of +0.026 on C(1) and a larger one of +0.876 on Xe in comparison to +0.440 and +0.391, respectively, for **8**, the unfluorinated analogue of **6**. In contrast, the negative π charge is higher on C(1) in **6** (−0.265) than in **8** (−0.205). In both cases the π charge on Xe can be neglected. The negative π charge on C(1) in combination with the positive σ charge on Xe strengthens electrostatically the C−Xe bond in **6**. On the other hand, the high positive σ charge on C(1) and Xe in **8** weakens the C−Xe bond. Consequently the calculated C−Xe distance is significantly shorter in **6** (2.16 Å) than in **8** (2.55 Å). **8** presents an intermediate situation between a covalent bond and a van der Waals interaction between the phenyl cation **9** and Xe°. As

(16) Frost, D. C.; McDowell, C. A. *Can. J. Chem.* **1958**, *36*, 39.
(17) Watanabe, K. *J. Chem. Phys.* **1957**, *26*, 542.
(18) Leech, H. R. In *Mellor's Comprehensive Treatise on Inorganic and Theoretical Chemistry*; Wiley: New York, 1956; Vol. 2, Suppl. 1, p 85.

Table 5. ^{19}F and ^{129}Xe NMR Chemical Shifts (δ/ppm) and $^3J(F-Xe)$ Coupling Constants ($^3J(F-Xe)$/Hz) of $[C_6F_5Xe][AsF_6]$ in Different Solvents

	^{19}F NMR					^{129}Xe NMR				
solvent	T/°C	δ F(2,6)	δ F(4)	δ F(3,5)	$^3J(F-Xe)$	T/°C	δ Xe	DN	AN	ϵ (T/°C)
H_2O	35	−126.47	−142.53	−154.69	69.1	24	−3862.3	18.0[11]	54.8[11]	80.4 (20)[12]
MeCN	35	−124.75	−141.27	−154.20	67.3	24	−3826.2	18.9[11]	14.1[11]	37.5 (20)[12]
TFE	0	−124.54	−140.06	−153.06	62.9	–	–	–	53.3[11]	25.6 (20)[16]
SO_2	0	−124.56	−139.61	−152.83	57.0	−40	−3903.0	–	–	17.3 (−30)[17]
AHF	−10	−123.08	−137.79	−151.47	58.9	−10	−3967.5	–	–	83.6 (0)[18]

Table 6. Calculated (LANL2DZ/RHF) Total Energies, Selected Geometrical Parameters, and Charge Densities (Mulliken and Natural Population Analysis) of Aryl- and Alkyl-Xe Cations

				distance/Å	angle/deg	charge density of Xe			charge density of C(1)		
compound		symmetry	HF/kJ mol^{-1}	Xe−C(1)	C(2)−C(1)−C(6)	σ nc[a]	π nc	Mc[b]	σ nc	π nc	Mc
$[C_6F_5Xe]^+$	**6**	C_s	−1 939 986.8	2.16	122.7	0.876	0.014	0.886	0.026	−0.265	−0.870
$[C_6F_5Xe][AsF_6]$[d]	**5**	C_s	−3 522 614.7	2.12	121.3	1.061[c]		1.083	−0.331[c]		−1.032
$[C_6H_5Xe]^+$	**8**	C_s	−642 898.7	2.55	135.1	0.391	0.005	0.409	0.440	−0.205	0.003
$[2,6\text{-}C_6H_3F_2Xe]^+$	**10**	C_s	−1 161 762.2	2.19	123.0	0.798	0.011	0.794	0.065	−0.284	−0.740
$[C_6F_5]^+$	**7**	C_s	−1 899 833.0	–	139.3		–		0.833	−0.258	0.305
$[C_6H_5]^+$	**9**	C_s	−602 917.4	–	144.6		–		0.765	−0.163	0.466
$[CF_3Xe]^+$ [e]	**11**	C_1	−921 201.8	3.48	–	0.032[c]		0.067	1.655[c]		1.016
$[CH_3Xe]^+$ [f]	**12**	C_1	−142 957.3	2.58	–	0.360[c]		0.385	−0.122[c]		−0.358

[a] nc = natural charge. [b] Mc = Mulliken charge. [c] Sum of σ and π natural charge. [d] Charge on $F_b = -0.731$, $F_{eq} = -0.678$ (average), distance Xe−F_b = 2.56 Å, angle Xe−F_b−As = 118.7°. [e] Angle C(1)−Xe−F = 91.2°, F−C−F = 120.0°. [f] Angle Xe−C−H = 96.2°, H−C−H = 118.9°.

Table 7. Calculated (LANDL2DZ/RHF) Total Energies, Selected Geometrical Parameters, and Charge Densities (Mulliken and Natural Population Analysis) of $[C_6F_5\text{-}Ng]^+$ Cations

				distance/Å	angle/deg	charge density of Ng			charge density of C(1)		
cation		symmetry	HF/kJ mol^{-1}	Ng−C(1)	C(2)−C(1)−C(6)	σ nc[a]	π nc	Mc[b]	σ nc	π nc	Mc
$[C_6F_5Xe]^+$	**6**	C_s	−1 939 986.8	2.16	122.7	0.876	0.014	0.886	0.026	−0.265	−0.870
$[C_6F_5Kr]^+$	**13a**	C_s	−1 946 838.8	2.06	126.0	0.622	0.009	0.583	0.257	−0.282	−0.519
$[C_6F_5Ar]^+$	**13b**	C_s	−1 954 154.3	2.06	130.2	0.389	0.006	0.350	0.471	−0.287	−0.146
$[C_6F_5Ne]^+$	**13c**	C_s	−2 237 212.3	2.29	138.5	0.038	0.001	0.045	0.796	−0.267	−0.267
$[C_6F_5Ne]^+$ [c]	**13c**	C_s	−2 237 098.4	2.07	137.5	0.072	0.002	0.067	0.769	−0.272	0.298
$[C_6F_5He]^+$ [c]	**13d**	C_s	−1 907 333.0	2.01	138.4	0.229	0.000	0.054	0.649	−0.334	0.238
$[C_6F_5He]^+$ [d]	**13d**	C_s	−1 907 652.7	1.33	132.8	0.288[e]		0.176	0.189[e]		−0.003

[a] nc = natural charge. [b] Mc = Mulliken charge. [c] Basis set: LANL2DZ on carbon and fluorine, 6-31G on Ng. [d] Basis set: 6-31G**. [e] Sum of σ and π natural charge.

can be seen in Table 6, the shift of positive σ charge from Xe to C(1) of the aromatic group correlates with a significant increase of the angle C(2)−C(1)−C(6). This angle reaches a maximum value in the aryl cations **7** and **9**. In alkylxenonium cations there is no polarizable π system which could stabilize the C−Xe bond by electrostatic interaction. As a consequence the positive charge in $[MeXe]^+$, **12** is mainly located on the three H atoms, whereas the C atom acquires a small negative charge of −0.123. The small Xe−C−H angle of 96.2° shows that the alkyl group has substantial cationic character, which means that the methyl cation polarizes Xe°. Perfluorination of the methyl group as in **10** causes a high positive charge on carbon (+1.655) combined with small positive charge on Xe (+0.032). The C−Xe distance indicates only a weak van der Waals interaction, whereas in $[MeXe]^+$ the C−Xe distance is 36% shorter than the sum of the van der Waals radii.

Due to the electron-poor σ backbone and the polarizable π system, the C_6F_5 group appears to be an optimal ligand in organoxenonium cations. Our calculations show that the C−Xe bond in **6** is 172.5 kJ/mol more stable than in **8**.

To study how the C−Ng bond changes with the nature of the noble gas, we carried out also calculations for the cations $[C_6F_5Ng]^+$ of the lighter noble gases Ng. The results (Table 7) reveal that significant changes are observed for the σ part of the bond, while the changes in the π system are only minor.

Thus, in $[C_6F_5Ng]^+$ the σ charge on Ng decreases from +0.876 in Xe to +0.038 in Ne; at the same time, the σ charge on C(1) increases from 0.026 to 0.796 and the angle C(2)−C(1)−C(6) increases from 122.7 to 138.5°. The charge distribution and geometrical data for $[C_6F_5Kr]^+$ suggest that salts with this cation could exist in the gas phase. However, due to the high oxidative strength of KrF_2, C_6F_5 transfer reagents such as $B(C_6F_5)_3$ are not feasible for the synthesis of $[C_6F_5Kr]^+$.

According to the ab initio calculations the change of the charge distribution in going from the cation **6** to the salt **5** is similar to the one going from the cation $[FXe]^+$ (**4**) to the hypervalent molecule XeF_2 (**1**). In the latter case, the natural charge on Xe becomes slightly more positive (from +1.284 to +1.331) and the F atoms become significantly more negative (from −0.284 to −0.666). In the former, the charge on Xe goes from 0.890 to 1.061, the charge on C(1) from −0.239 to −0.331, and the angle C(2)−C(1)−C(6) decreases from 122.7 to 121.3°. The fluorine bridge F_b between the strongly electrophilic cation and the weak nucleophilic anion is part of a linear, asymmetric hypervalent arrangement of the Xe center with a 118.7° Xe−F_b−As angle (Xe−F_b 2.56 Å). The As−F_t distance (1.73 Å) for the F atom trans to F_b is significantly shorter than the As−F_b distance (1.82 Å) and slightly shorter than the four equatorial As−F distances (average 1.75 Å). F_b carries a higher negative charge than all other As-bonded F

atoms. Our calculations suggest that more nucleophilic fluoroelementate anions than $[AsF_6]^-$ when interacting with **6** will establish a higher negative σ charge on C(1) and a higher positive σ charge on Xe and will therefore favor electron transfer from C(1) to Xe(II), thereby destabilizing the compound. With the same argument we can explain the reactions between **5** and CsF in MeCN described earlier.[14] The homolytic cleavage of the C−Xe bond proceeds due to the interaction with the strong nucleophilic fluoride anion.

$$[C_6F_5Xe][AsF_6] + CsF \rightarrow$$

$$Cs[AsF_6]\downarrow + \langle C_6F_5XeF\rangle \rightarrow C_6F_5^{\bullet} + {}^{\bullet}XeF \quad (7a)$$

$$C_6F_5^{\bullet} \xrightarrow{MeCN} C_6F_5H + (C_6F_5)_2 \quad (7b)$$

The unexpected long $Xe-F_b$ distance in $[2,6\text{-}C_6H_3F_2Xe][BF_4]$ can be rationalized by the higher transfer of positive charge from Xe to the H-containing aryl group in $[2,6\text{-}C_6H_3F_2Xe]^+$ (**10**) compared to **6**. Despite the higher nucleophilicity of $[BF_4]^-$ relative to $[AsF_6]^-$ the cation−anion interaction is weaker because of the lower σ charge (0.798) on Xe in $[2,6\text{-}C_6H_3F_2\text{-}Xe]^+$.

Acknowledgment. This work was supported by the Deutsche Forschungsgemeinschaft and the Fonds der Chemischen Industrie.

Supporting Information Available: Experimental details of the crystal structure determination (Table S1), atomic coordinates and coefficients of the equivalent isotropic temperature factors (Table S2), and distances and angles of **5** (Table S3) are available (4 pages). Ordering information is given on any current masthead page.

IC9801903